JOURNAL OF GUIDANCE, CONTROL, AND DYNAMICS
Vol. 23, No. 4, July–August 2000

Generalization of Foreshortening Through New Reduced Geometrically Nonlinear Structural Formulation

Javier Urruzola,* Juan Tomás Celigüeta,† and Javier García de Jalón‡
University of Navarre, 20009 Gipuzkoa, Spain

A new reduced formulation for modeling elastic structures or structural components with geometric nonlinearities is presented. This formulation is obtained as a generalization of the concept of foreshortening, which has been successfully used by other authors to model beams. Some examples are provided that illustrate the generality and validity of this formulation. The proposed theory is compared to previous work related to foreshortening, variable reduction in nonlinear elastic problems, and the use of a geometric stiffness matrix. Some guidelines are also given to implement the proposed method and to interpret the concepts that it involves. The reduction method presented is general, but a corotational approach is followed to simplify the exposition.

I. Introduction

THE analysis of elastic structures with geometric nonlinearities is of interest in a large number of fields of application and research. An example of this are space structures, in which the need for minimum weight obliges designers to reduce the thickness of the structural components, which results in the appearance of large deflections.[1] Structural members belonging to ship and aerospace structures also suffer this limitation in weight, and, as a consequence, the hull of an aircraft must resist stresses in the range of large deflections of plates and shells (when the deflections are of the same order as the thickness or larger[2]). As a last example, one can mention the analysis of any element whose failure can be caused by elastic unstability.[3]

One point to consider when tackling a structural analysis problem with a certain degree of geometrical complexity is the large number of variables required to model the structure [usually by means of a finite element method (FEM) program] and, consequently, the high demand for computational resources. This situation becomes aggravated in nonlinear problems by the need to iterate and to calculate Jacobians. For these reasons, a reduction in the number of configuration variables is clearly of interest in these problems. This reduction has been very successfully achieved in linear problems (modal analysis) but not as much in nonlinear problems. Among the methods proposed in the literature mention can be made of those by Noor and Peters[4] (differentiation with respect to force parameters), Idelsohn and Cardona[5] (modal derivatives and pseudomodal derivatives based on the stiffness matrix), and Slaats et al.[6] (modal derivatives and static modes).

In addition, another problem that has aroused considerable attention in the last few years is that of geometric stiffening of slender structural members subjected to large angular velocities.[7–9] To solve this problem in beams, several alternatives have been proposed, such as the use of a beam stretch variable instead of the axial displacement,[7] the use of a geometric stiffness matrix,[8] and the modelization of the nonlinear behavior through a set of modal amplitudes obtained in the linear modal analysis.[10] Banerjee and Kane[11] have also presented a formulation for plates under the restrictive assumption of inextensibility of the neutral plane.

The use of the foreshortening[9] is another method that has been proposed to solve this problem. This interesting concept provides certain important calculation advantages despite that, unfortunately, it has been impossible to generalize structural members other than cantilever beams. The present paper develops a generalization of the concept of foreshortening that can be applied to any type of structure or structural component with elastic behavior and geometric nonlinearities.

The result is a method of structural analysis with variable reduction that provides considerable savings in calculation times, as well as an interesting theoretical model for the purpose of studying these types of problems analytically. In addition, the presented derivation allows a better understanding of the relationships between the different approaches that are used to solve the geometric stiffening problem.[9]

This paper is organized as follows. First, a brief introduction to the foreshortening concept is presented (Sec. II). This is followed by a second-order corotational formulation of elastic structural analysis including geometric nonlinearities that provide an easy introduction to the ideas presented (Sec. III). Next, foreshortening is redefined and generalized in the framework of the structural formulation just mentioned, up to a new reduced formulation of the nonlinear problem (Sec. IV). This derivation is subsequently refined, and relevant terms are identified and interpreted (Sec. V). A brief description of the particularization of the proposed formalism in the case of a planar cantilever beam (Sec. VI) and the key steps of the numerical algorithm of the static problem (Sec. VII) are subsequently included. In Sec. VII, it is also explained how to use the presented formulation to generate reduced component models valid for multibody analysis. In the succeeding section, the most relevant connections with other derivations where foreshortening or variable reduction are applied are discussed. Finally, some examples are provided that illustrate the potential of this theory (Sec. IX).

II. Brief Introduction to the Concept of Foreshortening

In this section an explanation of foreshortening is given that roughly encompasses the ideas to be found in Ref. 9. As an initial step, an example is studied that has become both a benchmark and the first example to try in the work of the authors involved in the research on foreshortening: the rotating beam (see Fig. 1). This rotating beam has its origin in all probability in the normal working conditions of a helicopter rotor blade, which is a slender element that rotates at high speed. It is well known that the bending stiffness to be found in this element (in the normal working conditions it allows the blade to keep a straight configuration in spite of the aerodynamic friction forces) is due not only to its elastic properties, but also to the centrifugal force. This force tends to keep the blade aligned with the radial direction.

The problem is that this behavior that both experimentally and intuitively is certain is not reflected in a simulation that models the

Received 15 March 1999; revision received 25 November 1999; accepted for publication 30 November 1999.

*Postdoctoral Research Assistant, Applied Mechanics Department, Centro de Estudios e Investigaciones Técnicas de Guipúzcoa, P° Manuel Lardizabal, 15, Apdo, 20009, San Sebastian, Spain; jurruzola@ceit.es.

†Area Head, Applied Mechanics Department, Centro de Estudios e Investigaciones Técnicas de Guipúzcoa, P° Manuel Lardizabal, 15, Apdo, 20009, San Sebastian, Spain; jtceligueta@ceit.es.

‡Professor of Computer Science, Faculty of Industrial Engineering, P° Manuel Lardizabal, 13, Apdo, 20009, San Sebastian, Spain; jgjalon@ceit.es.

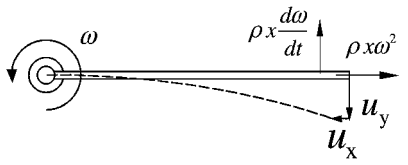

Fig. 1 Rotating beam.

beam with a linear elasticity formulation. This is because in a linear formulation the beam deflections are perpendicular to the straight line that corresponds to its undeformed configuration ($\boldsymbol{u}_y$ Fig. 1). However, when second-order effects are considered, a first-order transversal deflection causes a second-order stretch of the beam. To compensate this stretch, the deflections must have a component $\boldsymbol{u}_x$ (Fig. 1) that tends to retract the beam in the axial direction since beams usually have a very high axial stiffness (most times they can be considered to be inextensible). The result is that in a linear formulation the axial deformation is zero, whereas in a higher-order one it counteracts the centrifugal force, thereby generating negative work and providing the desired stabilizing effect (Fig. 1).

Once it has been shown that this shortening suffered by the beam, commonly known as foreshortening, causes this behavior, it becomes necessary to calculate it. One way of doing this is to apply the inextensibility hypothesis, so that the transverse deflections are complemented by longitudinal contractions that keep the extension zero.

If $\boldsymbol{u}_y$ is defined as the transverse deflection, $\boldsymbol{u}_x$ as the axial deflection, X as the undeformed axial coordinate of a generic point of the beam that is measured from its clamped end, and s as the beam length coordinate that is also measured from the same point, it holds that

$$\mathrm{d}s = \left[(\mathrm{d}X + \mathrm{d}\boldsymbol{u}_x)^2 + \mathrm{d}\boldsymbol{u}_y^2\right]^{\frac{1}{2}} \approx \mathrm{d}X\left[1 + \frac{\mathrm{d}\boldsymbol{u}_x}{\mathrm{d}X} + \frac{1}{2}\left(\frac{\mathrm{d}\boldsymbol{u}_y}{\mathrm{d}X}\right)^2\right] \tag{1}$$

and the inextensibility condition can be expressed as

$$\frac{\mathrm{d}\boldsymbol{u}_x}{\mathrm{d}X} = -\frac{1}{2}\left(\frac{\mathrm{d}\boldsymbol{u}_y}{\mathrm{d}X}\right)^2 \tag{2}$$

which makes it possible to obtain the axial deflection $\boldsymbol{u}_x$ as a function of the transverse deflection $\boldsymbol{u}_y$.

If the transverse displacements and rotations are expressed with the aid of a modal matrix $\boldsymbol{\Phi}$ and a set of modal amplitudes $\boldsymbol{\theta}$, the axial deflection for an arbitrary point of the beam whose undeformed axial coordinate is X can be written as

$$\boldsymbol{u}_x(X) = \int_0^X \left[-\frac{1}{2}\left(\frac{\mathrm{d}\boldsymbol{u}_y}{\mathrm{d}X}\right)^2\right]\mathrm{d}X = \int_0^X \left[-\frac{1}{2}\left(\frac{\mathrm{d}\boldsymbol{\Phi}_y}{\mathrm{d}X}\boldsymbol{\theta}\right)^2\right]\mathrm{d}X$$

$$= \int_0^X \left(-\frac{1}{2}(\boldsymbol{\Phi}_\theta\boldsymbol{\theta})^2\right)\mathrm{d}X \tag{3}$$

where $\boldsymbol{\Phi}_y$ is the modal matrix associated with the transverse deflections, whereas $\boldsymbol{\Phi}_\theta = \mathrm{d}\boldsymbol{\Phi}_y/\mathrm{d}X$ corresponds to the angular deformation.

III. Simple and Intuitive Formulation of Elastic Structural Analysis Including Geometric Nonlinearities

A. Preliminary Conventions

To understand the following conventions more easily, we can introduce the matrix $\boldsymbol{\Phi}$, whose columns are the modes of the generic structure to be treated in this formulation. It is assumed that the structure is modeled following the FEM approach. In addition, each node of the structure is supposed to have six configuration variables associated with it: three rotations and three translations. $\boldsymbol{\Phi}_r$ is the part of $\boldsymbol{\Phi}$ corresponding to the rotational nodal coordinates (angles), whereas $\boldsymbol{\Phi}_t$ is the part of $\boldsymbol{\Phi}$ corresponding to the translational nodal coordinates. The vector $\boldsymbol{\theta}$ contains the modal amplitudes associated with the modes in $\boldsymbol{\Phi}$.

Index E is used to represent the part of a magnitude corresponding to the nodal coordinates of a generic finite element E. For example, K_E is the stiffness matrix of element E, whereas K is the stiffness matrix of the structure. Index $\bar{E}$ is used for representing a matrix or vector obtained from the corresponding matrix or vector with index E by calculating the mean of the submatrices or subvectors corresponding to each node on the element E and replacing the values corresponding to each node by the mean values subsequently.

Δ followed by index E is the result of substracting the quantity with index $\bar{E}$ from the quantity with index E, for example, $\Delta\boldsymbol{\Phi}_E = \boldsymbol{\Phi}_E - \boldsymbol{\Phi}_{\bar{E}}$. In other words this notation is used for representing deviations of nodal measures with respect to the average nodal measure in the generic element E.

A formula such as $\boldsymbol{\Phi}_r\boldsymbol{\theta} \times \boldsymbol{\Phi}_t\boldsymbol{\theta}$ means: take the three-component subvectors associated with each node that are contained in the vectors $\boldsymbol{\Phi}_r\boldsymbol{\theta}$ and $\boldsymbol{\Phi}_t\boldsymbol{\theta}$ and calculate a cross product for each pair of subvectors corresponding to the same node; then form a new vector by assembling the resultant three-component vectors.

B. Formulation of Structural Analysis

One of the purposes of the formulation presented is to employ the familiar concepts of the FEM when applied to linear elasticity problems. Concepts such as the element stiffness matrix associated with a finite element or that of the structure as well as other familiar concepts from the modal analysis will be used.

To represent the structure configuration, the nodal coordinate vector $\boldsymbol{u}$ as well as the modal amplitude vector $\boldsymbol{\theta}$ can be used on condition that the whole set of modes is considered for analysis. This is so because the columns of matrix $\boldsymbol{\Phi}$ form a basis of the configuration space of the structure. Its configuration can, therefore, be represented either by $\boldsymbol{u}$ or by $\boldsymbol{\theta}$:

$$\boldsymbol{u} = \boldsymbol{\Phi}\boldsymbol{\theta} \tag{4}$$

$$\boldsymbol{\theta} = \boldsymbol{\Phi}^{-1}\boldsymbol{u} \tag{5}$$

The second key idea of this formulation is straightforward: As a structure increases its deformation, the orientation of each finite element changes relative to the structure frame. This causes the deformations measured in the structure frame to differ more and more from those to be measured in a frame that follows the movement of every single element. It is, therefore, a good idea to transform the displacements from the structure frame to an element frame so that the elastic energy can be calculated with those local deformations for which the element stiffness matrix is certainly a good approximation. This approach can be regarded as being derived from the corotational approach[12,13] or the geometric nonlinear substructuring method.[14]

However, in contrast to the aforementioned substructuring approach, instead of using a frame with its own coordinates for each finite element, in the subsequent derivations the corotational frame will be located by operating on the values of the configuration variables $\boldsymbol{u}$ or $\boldsymbol{\theta}$. For example, in the case of a beam (Fig. 2) the rotation part of the nodal coordinate set $\boldsymbol{\Phi}_r\boldsymbol{\theta}$ gives the angular orientation of the centroidal line at each node, and this is enough information to calculate the orientation of a nodal-bound frame. Consequently, the mean of the orientations of all of the nodes that compose an element ($\overline{\boldsymbol{\Phi}_{rE}\boldsymbol{\theta}}$) can be thought of as the orientation of the intended element corotational frame (see the Appendix for the case in which the structure model does not provide orientations). Analogously, by taking the mean of the deformed translational coordinates of the element nodal set, the location of a point that is appropriate to be selected as the origin of the corotational frame can be obtained ($\overline{\boldsymbol{\Phi}_{tE}\boldsymbol{\theta}}$).

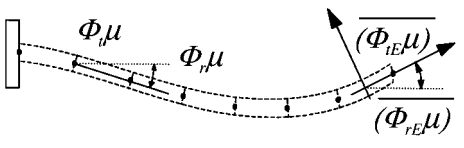

Fig. 2 Corotational approach for a beam.

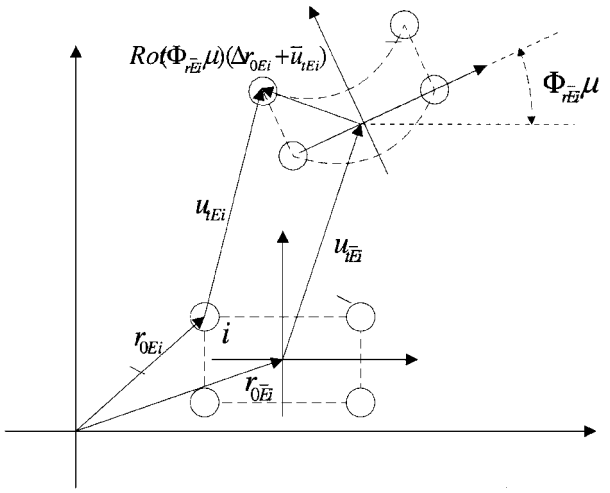

Fig. 3 Transformation of deformations to the element corotational frame.

Once both the orientation and position of each element frame are known, it is necessary to express the nodal displacements of each element in the element frame with the mentioned aim of using the element stiffness matrix in a frame where the linearity assumption is accurate enough. In the subsequent derivation, the nodal deformations of a generic element E expressed in the structure frame will be denoted $\boldsymbol{u}_E$, whereas $\bar{\boldsymbol{u}}_E$ will correspond to the same quantities expressed in the element frame (analogously the translational parts, $\boldsymbol{u}_{tE}$ and $\bar{\boldsymbol{u}}_{tE}$, and the rotational parts $\boldsymbol{\theta}_E$ and $\bar{\boldsymbol{\theta}}_E$).

The translational deformations of a generic node i of a generic element E expressed in the structure frame $\boldsymbol{u}_{tEi}$ and expressed in the element frame $\bar{\boldsymbol{u}}_{tEi}$ are related by the following expression (see Fig. 3):

$$r_{0\bar{E}i} + \boldsymbol{u}_{t\bar{E}i} + \mathrm{Rot}(\boldsymbol{\Phi}_{r\bar{E}i}\boldsymbol{\theta})(\Delta r_{0Ei} + \bar{\boldsymbol{u}}_{tEi}) = r_{0Ei} + \boldsymbol{u}_{tEi} \tag{6}$$

where r_0 contains the undeformed coordinates of the nodes of the structure and $\mathrm{rot}(\boldsymbol{\theta})$ is the rotation matrix associated with the rotation vector $\boldsymbol{\theta}$. Equation (6) can be solved for the corotational displacement $\bar{\boldsymbol{u}}_{tEi}$,

$$\bar{\boldsymbol{u}}_{tEi} = \mathrm{Rot}(\boldsymbol{\Phi}_{r\bar{E}i}\boldsymbol{\theta})^{-1}(\Delta\boldsymbol{\Phi}_{tEi}\boldsymbol{\theta} + \Delta r_{0Ei}) - \Delta r_{0Ei} \tag{7}$$

$$\bar{\boldsymbol{u}}_{tEi} \cong \left(I - \tilde{\boldsymbol{\Phi}}_{r\bar{E}i}\boldsymbol{\theta} + \tfrac{1}{2}\tilde{\boldsymbol{\Phi}}_{r\bar{E}i}\boldsymbol{\theta}\tilde{\boldsymbol{\Phi}}_{r\bar{E}i}\boldsymbol{\theta}\right)(\Delta\boldsymbol{\Phi}_{tEi}\boldsymbol{\theta} + \Delta r_{0Ei}) - \Delta r_{0Ei} \tag{8}$$

$$\bar{\boldsymbol{u}}_{tEi} \cong \Delta\boldsymbol{\Phi}_{tEi}\boldsymbol{\theta} - \boldsymbol{\Phi}_{r\bar{E}i}\boldsymbol{\theta} \times \Delta\boldsymbol{\Phi}_{tEi}\boldsymbol{\theta} - \boldsymbol{\Phi}_{r\bar{E}i}\boldsymbol{\theta} \times \Delta r_{0Ei} + \tfrac{1}{2}\boldsymbol{\Phi}_{r\bar{E}i}\boldsymbol{\theta} \times \boldsymbol{\Phi}_{r\bar{E}i}\boldsymbol{\theta} \times \Delta r_{0Ei} \tag{9}$$

To transform Eq. (7) into Eq. (8), the second-order approximation of the inverse of the rotation matrix of the element frame was used ($\tilde{\boldsymbol{\Phi}}_{r\bar{E}i}\boldsymbol{\theta}$ is the antisymmetric matrix associated to vector $\boldsymbol{\Phi}_{r\bar{E}i}\boldsymbol{\theta}$)

$$\mathrm{Rot}(\boldsymbol{\Phi}_{r\bar{E}i}\boldsymbol{\theta})^{-1} \cong I - \tilde{\boldsymbol{\Phi}}_{r\bar{E}i}\boldsymbol{\theta} + \tfrac{1}{2}\tilde{\boldsymbol{\Phi}}_{r\bar{E}i}\boldsymbol{\theta}\tilde{\boldsymbol{\Phi}}_{r\bar{E}i}\boldsymbol{\theta} \tag{10}$$

Moreover, terms of order higher than two were neglected to transform Eq. (8) into Eq. (9).

By the applying of the conventions presented in Sec. III.A, Eq. (9) can be extended to express the corotational deformation of the whole set of nodes of the generic element E,

$$\bar{\boldsymbol{u}}_{tE} \cong \Delta\boldsymbol{\Phi}_{tE}\boldsymbol{\theta} - \boldsymbol{\Phi}_{r\bar{E}}\boldsymbol{\theta} \times \Delta\boldsymbol{\Phi}_{tE}\boldsymbol{\theta} - \boldsymbol{\Phi}_{r\bar{E}}\boldsymbol{\theta} \times \Delta r_{0E} + \tfrac{1}{2}\boldsymbol{\Phi}_{r\bar{E}}\boldsymbol{\theta} \times \boldsymbol{\Phi}_{r\bar{E}}\boldsymbol{\theta} \times \Delta r_{0E} \tag{11}$$

Analogously to Eq. (6), the angular deformations can be expressed in the element frame

$$\boldsymbol{\Phi}_{r\bar{E}}\boldsymbol{\theta} + \bar{\boldsymbol{\theta}}_E = \boldsymbol{\Phi}_{rE}\boldsymbol{\theta} \tag{12}$$

$$\bar{\boldsymbol{\theta}}_E = \Delta\boldsymbol{\Phi}_{rE}\boldsymbol{\theta} \tag{13}$$

If $A_E(x_E)$ represents an assembly function of a generic magnitude x [which can be used, for example, for assembling the element stiffness matrices into the structure stiffness matrix, i.e., $K = A_E(K_E)$], it is possible to write the elastic energy of the whole structure as the sum (or assembly) of the contributions of each element:

$$V = \underset{E}{A}(V_E) = \underset{E}{A}\left(\tfrac{1}{2}\bar{\boldsymbol{u}}_E^T K_E \bar{\boldsymbol{u}}_E\right) \tag{14}$$

This expression can be simplified if it is taken into account that a part of $\bar{\boldsymbol{\theta}}_E$ [Eq. (13)] and another of $\bar{\boldsymbol{u}}_{tE}$ [Eq. (11)] correspond to first-order rigid-body movements, namely,

$$\bar{\boldsymbol{u}}_{tE}^R = -\boldsymbol{\Phi}_{t\bar{E}}\boldsymbol{\theta} - \boldsymbol{\Phi}_{r\bar{E}}\boldsymbol{\theta} \times \Delta r_0 \tag{15}$$

$$\bar{\boldsymbol{\theta}}_E^R = -\boldsymbol{\Phi}_{r\bar{E}}\boldsymbol{\theta} \tag{16}$$

The remaining deformation terms, which will be denoted as $\bar{\boldsymbol{\theta}}_E^D$ and $\bar{\boldsymbol{u}}_{tE}^D$, can be expressed as

$$\bar{\boldsymbol{u}}_{tE}^D = \boldsymbol{\Phi}_{tE}\boldsymbol{\theta} - \boldsymbol{\Phi}_{r\bar{E}}\boldsymbol{\theta} \times \Delta\boldsymbol{\Phi}_{tE}\boldsymbol{\theta} + \tfrac{1}{2}\boldsymbol{\Phi}_{r\bar{E}}\boldsymbol{\theta} \times \boldsymbol{\Phi}_{r\bar{E}}\boldsymbol{\theta} \times \Delta r_0 \tag{17}$$

$$\bar{\boldsymbol{\theta}}_E^D = \boldsymbol{\Phi}_{rE}\boldsymbol{\theta} \tag{18}$$

Expression (17) can be simplified by approximating the displacement of each node of a finite element relative to the origin of the element frame by the rigid-body displacement caused by the rotation of the element frame

$$\Delta\boldsymbol{\Phi}_{tE}\boldsymbol{\theta} \cong \boldsymbol{\Phi}_{r\bar{E}}\boldsymbol{\theta} \times \Delta r_0 \tag{19}$$

so that Eq. (17) can be rewritten as

$$\bar{\boldsymbol{u}}_{tE}^D \cong \boldsymbol{\Phi}_{tE}\boldsymbol{\theta} - \tfrac{1}{2}\boldsymbol{\Phi}_{r\bar{E}}\boldsymbol{\theta} \times \Delta\boldsymbol{\Phi}_{tE}\boldsymbol{\theta} \tag{20}$$

Finally, if one bears in mind that the finite element must not generate deformation energy when it is subjected to first-order rigid-body movements, one can express the elastic energy of the structure as

$$V = \underset{E}{A}\left[\tfrac{1}{2}\left(\bar{\boldsymbol{u}}_E^D\right)^T K_E \bar{\boldsymbol{u}}_E^D\right] = \underset{E}{A}\left[\tfrac{1}{2}\left(\boldsymbol{\Phi}_E\boldsymbol{\theta} - \tfrac{1}{2}\boldsymbol{\Phi}_{r\bar{E}}\boldsymbol{\theta} \times \Delta\boldsymbol{\Phi}_E\boldsymbol{\theta}\right)^T \cdot K_E\left(\boldsymbol{\Phi}_E\boldsymbol{\theta} - \tfrac{1}{2}\boldsymbol{\Phi}_{r\bar{E}}\boldsymbol{\theta} \times \Delta\boldsymbol{\Phi}_E\boldsymbol{\theta}\right)\right] \tag{21}$$

where $\Delta\boldsymbol{\Phi}_E$ is considered to be zero for the rotational part of the nodal coordinates so that

$$\bar{\boldsymbol{u}}_E^D = \boldsymbol{\Phi}_E\boldsymbol{\theta} - \tfrac{1}{2}\boldsymbol{\Phi}_{r\bar{E}}\boldsymbol{\theta} \times \Delta\boldsymbol{\Phi}_E\boldsymbol{\theta} \tag{22}$$

is valid for both rotations and translations.

Note that the elastic energy could also be calculated using the Green–Lagrange tensor. This approach would also result in a fourth-order dependency of the elastic energy on the modal amplitudes, and the subsequently developed formulation would still be valid. Nevertheless, in this paper the presented corotational approach was preferred due to its simplicity.

IV. First Generalization of the Concept of Foreshortening: Independence of the Structure Shape

To obtain a concept of foreshortening that not only encompasses those existing in the literature but also is valid for structural elements other than beams, a distinction will be drawn between modes selected for the analysis (low natural frequencies) and nonselected modes (high natural frequencies) in a fashion similar to that of traditional modal analysis. It will be demonstrated that under certain conditions it is possible to express the values of the nonselected modal amplitudes explicitly as a function of the amplitudes of the selected modes, hence reducing the number of variables needed to model the nonlinear structure. The value of the nonselected modal amplitudes as a function of the selected set will be easily interpreted as a generalized foreshortening projected over the nonselected modes.

Hereafter, the modal amplitudes corresponding to high frequencies are ζ and the corresponding part of the modal matrix is ψ. In addition η and ϕ are the low-frequency amplitudes and modes, respectively. Consequently, the nodal displacements can be written as

$$\boldsymbol{u} = \boldsymbol{\Phi\theta} = \phi\eta + \psi\zeta \tag{23}$$

and the elastic energy in Eq. (21) as

$$V = \underset{E}{A}\left[\tfrac{1}{2}\left(\bar{\boldsymbol{u}}_E^D\right)^T K_E\left(\bar{\boldsymbol{u}}_E^D\right)\right]$$

$$\bar{\boldsymbol{u}}_E^D = (\phi_E\eta + \psi_E\zeta) - \tfrac{1}{2}(\phi_{r\bar{E}}\eta + \psi_{r\bar{E}}\zeta) \times (\Delta\phi_E\eta + \Delta\psi_E\zeta) \tag{24}$$

Note that the modal amplitudes ζ correspond to modes of such a high natural frequency that their contribution to the deformation in the linear analysis is negligible. Only when the deformations are large or stiffening effects appear are their values significant. Taking this into account, we introduce the following hypothesis: The high frequency modal amplitudes ζ can be considered only up to first order in the corotational displacements $\bar{\boldsymbol{u}}_E^D$ [see Eq. (24)]:

$$\bar{\boldsymbol{u}}_E^D \cong (\phi_E\eta + \psi_E\zeta) - \tfrac{1}{2}(\phi_{r\bar{E}}\eta) \times (\Delta\phi_E\eta) \tag{25}$$

We will call this hypothesis the generalized von Kármán hypothesis and will justify this name in Sec. VIII by relating this hypothesis to the von Kármán hypothesis for geometrically nonlinear plates. Employing Eq. (25), the energy in Eq. (21) can be written as

$$V = \underset{E}{A}\left\{\tfrac{1}{2}\left[\phi_E\eta + \psi_E\zeta - \tfrac{1}{2}(\phi_{r\bar{E}}\eta) \times (\Delta\phi_E\eta)\right]^T \cdot K_E\left[\phi_E\eta + \psi_E\zeta - \tfrac{1}{2}(\phi_{r\bar{E}}\eta) \times (\Delta\phi_E\eta)\right]\right\} \tag{26}$$

The elastic forces $Q_{\mathrm{el}\zeta}$ corresponding to the modal amplitudes ζ can now be obtained by taking derivatives in Eq. (26) with respect to ζ:

$$\begin{aligned} -Q_{\mathrm{el}\zeta} = \frac{\partial V}{\partial\zeta} &= \underset{E}{A}\left\{\psi_E^T K_E\left[\phi_E\eta + \psi_E\zeta - \tfrac{1}{2}(\phi_{r\bar{E}}\eta) \times (\Delta\phi_E\eta)\right]\right\} \\ &= \underset{E}{A}\left(\psi_E^T K_E\psi_E\zeta\right) + \underset{E}{A}\left\{\psi_E^T K_E\left[-\tfrac{1}{2}(\phi_{r\bar{E}}\eta) \times (\Delta\phi_E\eta)\right]\right\} \\ &= \psi^T K\psi\zeta + \psi^T \underset{E}{A}\left\{K_E\left[-\tfrac{1}{2}(\phi_{r\bar{E}}\eta) \times (\Delta\phi_E\eta)\right]\right\} \\ &= \Omega_\zeta^2\zeta + \psi^T \underset{E}{A}\left\{K_E\left[-\tfrac{1}{2}(\phi_{r\bar{E}}\eta) \times (\Delta\phi_E\eta)\right]\right\} \end{aligned} \tag{27}$$

where the modes ϕ and ψ are K-orthogonal; as a consequence of the properties of the assembly function, it is possible to place the vector ψ out of the assembly function argument; and the product $\psi^T K\psi = \underset{E}{A}\left(\psi_E^T K_E\psi_E\right)$ is a positive-definite diagonal matrix Ω_ζ^2 whose diagonal is composed of the natural frequencies associated with the modes ψ. After including the forces applied on the structure $Q_{\mathrm{ap}\zeta}$ projected over ζ in the analysis, the equilibrium equations for are obtained:

$$\Omega_\zeta^2\zeta + \psi^T \underset{E}{A}\left\{K_E\left[-\tfrac{1}{2}(\phi_{r\bar{E}}\eta) \times (\Delta\phi_E\eta)\right]\right\} = Q_{\mathrm{ap}\zeta} \tag{28}$$

The solution for the high-frequency modal amplitudes ζ can be expressed as the sum of two terms:

$$\zeta = \zeta' + \zeta_2 \tag{29}$$

where ζ_2 is obtained from the following equation as a quadratic (for this reason index 2 is used) function of the low-frequency modal amplitudes η

$$\Omega_\zeta^2\zeta_2 + \psi^T \underset{E}{A}\left\{K_E\left[-\tfrac{1}{2}(\phi_{r\bar{E}}\eta) \times (\Delta\phi_E\eta)\right]\right\} = 0 \tag{30}$$

Substituting the identity of Eq. (29) in Eq. (28), the equilibrium equations corresponding to the high-frequency amplitudes can be written as

$$\Omega_\zeta^2\zeta' = Q_{\mathrm{ap}\zeta} \tag{31}$$

which allows us to consider ζ' negligible with the same arguments as in the modal analysis (very high natural frequencies).

This suggests that the variable reduction can be achieved, if the dependency of the elastic energy on ζ is eliminated by substituting $\zeta_2 + \zeta'$ for ζ in Eq. (26) and ζ' is neglected. After substitution, V only depends on η because ζ_2 is a function of η from Eq. (30).

Moreover, it can be demonstrated (see Sec. VI) that the term $\psi\zeta_2$ calculated in this way coincides with the foreshortening when calculated for inextensible beams. Therefore, ζ_2 can be considered as a sort of generalized foreshortening projected over the nonselected modes. Intuitively, $\psi\zeta_2$ can be thought of as the response of the structure to eliminate the second-order deformation projected over the high-frequency modes that is caused by the first-order deformation in the low-frequency modes. Also ζ_2 can be regarded as the result of a second-order static condensation of the degrees of freedom of the structure.

V. Refinement and Interpretation of the Formalism

The ideas and derivations presented in the preceding section will be refined to obtain a systematic and numerically efficient formulation of the reduced structure model. This will allow a simple interpretation of the various terms that compose both the elastic energy and the kinematic description of an elastic structure with geometric nonlinearities. The starting point for this formulation is the extension of the concept of generalized foreshortening introduced in Sec. IV. For this purpose a new vector η_2, which can be regarded as a generalized foreshortening associated with the low-frequency amplitudes η, is defined using the following equation, which is a clear extension of Eq. (30) for the low-frequency spectrum:

$$\phi^T K\phi\eta_2 = -\phi^T \underset{E}{A}\left\{K_E\left[-\tfrac{1}{2}(\phi_{r\bar{E}}\eta) \times (\Delta\phi_E\eta)\right]\right\} \tag{32}$$

The vectors η_2 and ζ_2 can be collected in a single vector $\boldsymbol{\theta}_2$ as was done with η, ζ, and $\boldsymbol{\theta}$. Taking into account that the modes in $\boldsymbol{\Phi}$ are orthogonal, Eqs. (30) and (32) can be collected in a single equation:

$$\boldsymbol{\Phi}^T K\boldsymbol{\Phi\theta}_2 = -\boldsymbol{\Phi}^T \underset{E}{A}\left\{K_E\left[-\tfrac{1}{2}(\phi_{r\bar{E}}\eta) \times (\Delta\phi_E\eta)\right]\right\} \tag{33}$$

In the case of an inextensible beam, the selected modes occur only in the transversal direction. Therefore, η_2 is zero because it corresponds to the transversal part of the foreshortening, which is an axial deformation. Consequently, $\boldsymbol{\Phi\theta}_2$ coincides with $\psi\zeta_2$ in this case, and this allows us to consider $\boldsymbol{\Phi\theta}_2$ as a generalized foreshortening with the same arguments as in Sec. IV.

Similarly to the derivation for the high-frequency spectrum in the preceding section [see Eq. (29)], a new vector η' corresponding to the corrected low-frequency modal amplitudes can be defined by means of the following equation:

$$\eta = \eta' + \eta_2 \tag{34}$$

and the two sets of corrected modal amplitudes, η' and ζ' can be collected in a single vector $\boldsymbol{\theta}'$, for which the following identity holds:

$$\boldsymbol{\theta} = \boldsymbol{\theta}' + \boldsymbol{\theta}_2 \tag{35}$$

By the using of this relationship, the elastic energy in Eq. (26) can be expressed as

$$V = \underset{E}{A}\left\{\tfrac{1}{2}\left[\boldsymbol{\Phi}_E\boldsymbol{\theta}' + \boldsymbol{\Phi}_E\boldsymbol{\theta}_2 - \tfrac{1}{2}(\phi_{r\bar{E}}\eta) \times (\Delta\phi_E\eta)\right]^T \cdot K_E\left[\boldsymbol{\Phi}_E\boldsymbol{\theta}' + \boldsymbol{\Phi}_E\boldsymbol{\theta}_2 - \tfrac{1}{2}(\phi_{r\bar{E}}\eta) \times (\Delta\phi_E\eta)\right]\right\} \tag{36}$$

This expression can be rewritten more conveniently by repeatedly applying Eq. (33):

$$
\begin{aligned}
V = & \underset{E}{A}\left[\tfrac{1}{2}(\boldsymbol{\Phi}_E\boldsymbol{\theta}')^T K_E(\boldsymbol{\Phi}_E\boldsymbol{\theta}')\right] \\
& + \underset{E}{A}\left\{(\boldsymbol{\Phi}_E\boldsymbol{\theta}')^T K_E\left[\boldsymbol{\Phi}_E\boldsymbol{\theta}_2 - \tfrac{1}{2}(\boldsymbol{\phi}_{r\bar{E}}\boldsymbol{\eta})\times(\Delta\boldsymbol{\phi}_E\boldsymbol{\eta})\right]\right\} \\
& + \underset{E}{A}\left\{\tfrac{1}{2}(\boldsymbol{\Phi}_E\boldsymbol{\theta}_2)^T K_E\left[\boldsymbol{\Phi}_E\boldsymbol{\theta}_2 - \tfrac{1}{2}(\boldsymbol{\phi}_{r\bar{E}}\boldsymbol{\eta})\times(\Delta\boldsymbol{\phi}_E\boldsymbol{\eta})\right]\right\} \\
& + \underset{E}{A}\left\{\tfrac{1}{2}\left[-\tfrac{1}{2}(\boldsymbol{\phi}_{r\bar{E}}\boldsymbol{\eta})\times(\Delta\boldsymbol{\phi}_E\boldsymbol{\eta})\right]^T\right. \\
& \left.\cdot K_E\left[\boldsymbol{\Phi}_E\boldsymbol{\theta}_2 - \tfrac{1}{2}(\boldsymbol{\phi}_{r\bar{E}}\boldsymbol{\eta})\times(\Delta\boldsymbol{\phi}_E\boldsymbol{\eta})\right]\right\} \\
= & \underset{E}{A}\left[\tfrac{1}{2}\left(\boldsymbol{\Phi}_E\boldsymbol{\theta}'\right)^T K_E(\boldsymbol{\Phi}_E\boldsymbol{\theta}')\right] \\
& + \underset{E}{A}\left\{\tfrac{1}{2}\left[-\tfrac{1}{2}(\boldsymbol{\phi}_{r\bar{E}}\boldsymbol{\eta})\times(\Delta\boldsymbol{\phi}_E\boldsymbol{\eta})\right]^T\right. \\
& \left.\cdot K_E\left[\boldsymbol{\Phi}_E\boldsymbol{\theta}_2 - \tfrac{1}{2}(\boldsymbol{\phi}_{r\bar{E}}\boldsymbol{\eta})\times(\Delta\boldsymbol{\phi}_E\boldsymbol{\eta})\right]\right\} \\
= & \tfrac{1}{2}\boldsymbol{\theta}'^T\boldsymbol{\Phi}^T K\boldsymbol{\Phi}\boldsymbol{\theta}' + \underset{E}{A}\left\{\tfrac{1}{2}\left[-\tfrac{1}{2}(\boldsymbol{\phi}_{r\bar{E}}\boldsymbol{\eta})\times(\Delta\boldsymbol{\phi}_E\boldsymbol{\eta})\right]^T\right. \\
& \left.\cdot K_E\left[-\tfrac{1}{2}(\boldsymbol{\phi}_{r\bar{E}}\boldsymbol{\eta})\times(\Delta\boldsymbol{\phi}_E\boldsymbol{\eta})\right]\right\} - \tfrac{1}{2}\boldsymbol{\theta}_2^T\boldsymbol{\Phi}^T K\boldsymbol{\Phi}\boldsymbol{\theta}_2
\end{aligned}
\tag{37}
$$

Because of the orthogonality of the modes, it holds that

$$
\tfrac{1}{2}\boldsymbol{\theta}'^T\boldsymbol{\Phi}^T K\boldsymbol{\Phi}\boldsymbol{\theta}' = \tfrac{1}{2}\boldsymbol{\eta}'^T\boldsymbol{\phi}^T K\boldsymbol{\phi}\boldsymbol{\eta}' + \tfrac{1}{2}\boldsymbol{\zeta}'^T\boldsymbol{\psi}^T K\boldsymbol{\psi}\boldsymbol{\zeta}' \tag{38}
$$

This allows us to split the elastic energy V into two terms, V_1 and V_2,

$$
\begin{aligned}
V_1 = & \tfrac{1}{2}\boldsymbol{\eta}'^T\boldsymbol{\phi}^T K\boldsymbol{\phi}\boldsymbol{\eta}' + \underset{E}{A}\left\{\tfrac{1}{2}\left[-\tfrac{1}{2}(\boldsymbol{\phi}_{r\bar{E}}\boldsymbol{\eta})\times(\Delta\boldsymbol{\phi}_E\boldsymbol{\eta})\right]^T\right. \\
& \left.\times K_E\left[-\tfrac{1}{2}(\boldsymbol{\phi}_{r\bar{E}}\boldsymbol{\eta})\times(\Delta\boldsymbol{\phi}_E\boldsymbol{\eta})\right]\right\} - \tfrac{1}{2}\boldsymbol{\theta}_2^T\boldsymbol{\Phi}^T K\boldsymbol{\Phi}\boldsymbol{\theta}_2
\end{aligned}
\tag{39}
$$

$$
V_2 = \tfrac{1}{2}\boldsymbol{\zeta}'^T\boldsymbol{\psi}^T K\boldsymbol{\psi}\boldsymbol{\zeta}' \tag{40}
$$

Now we can make a change of variables and use as configuration variables $\boldsymbol{\eta}$ and $\boldsymbol{\zeta}'$. As a result, $\boldsymbol{\zeta}'$ and $\boldsymbol{\eta}$ are decoupled in the elastic energy because V_2 only depends on $\boldsymbol{\zeta}'$ and V_1 only depends on $\boldsymbol{\eta}$. The latter is because $\boldsymbol{\eta}'$ and $\boldsymbol{\theta}_2$ are functions only of $\boldsymbol{\eta}$ [see Eqs. (32) and (34) for $\boldsymbol{\eta}'$, and Eq. (33) for $\boldsymbol{\theta}_2$]. Taking derivatives of V_1 plus V_2 with respect to $\boldsymbol{\zeta}'$ results in the equilibrium equations associated to the high-frequency spectrum [Eq. (31)], which allowed us to consider $\boldsymbol{\zeta}'$ negligible.

After neglecting $\boldsymbol{\zeta}'$, the elastic energy in Eq. (37) can be expressed as

$$
\begin{aligned}
V \cong V_1 = & \tfrac{1}{2}\boldsymbol{\eta}'^T\boldsymbol{\phi}^T K\boldsymbol{\phi}\boldsymbol{\eta}' + \underset{E}{A}\left\{\tfrac{1}{2}\left[-\tfrac{1}{2}(\boldsymbol{\phi}_{r\bar{E}}\boldsymbol{\eta})\times(\Delta\boldsymbol{\phi}_E\boldsymbol{\eta})\right]^T\right. \\
& \left.\cdot K_E\left[-\tfrac{1}{2}(\boldsymbol{\phi}_{r\bar{E}}\boldsymbol{\eta})\times(\Delta\boldsymbol{\phi}_E\boldsymbol{\eta})\right]\right\} - \tfrac{1}{2}\boldsymbol{\theta}_2^T\boldsymbol{\Phi}^T K\boldsymbol{\Phi}\boldsymbol{\theta}_2
\end{aligned}
\tag{41}
$$

By taking into account that $\boldsymbol{\Phi}$ is a basis of the configuration space, it is possible to transform Eq. (33) into

$$
K\boldsymbol{u}_2 = -\underset{E}{A}\left\{K_E\left[-\tfrac{1}{2}(\boldsymbol{\phi}_{r\bar{E}}\boldsymbol{\eta})\times(\Delta\boldsymbol{\phi}_E\boldsymbol{\eta})\right]\right\} \tag{42}
$$

where $\boldsymbol{u}_2 = \boldsymbol{\Phi}\boldsymbol{\theta}_2$ is the generalized foreshortening projected over the nodal coordinates. By the substituting of the nodal foreshortening $\boldsymbol{u}_2$ for the modal foreshortening $\boldsymbol{\theta}_2$ in Eq. (41), a new expression of the elastic energy is obtained:

$$
\begin{aligned}
V = & \tfrac{1}{2}\boldsymbol{\eta}'^T\boldsymbol{\phi}^T K\boldsymbol{\phi}\boldsymbol{\eta}' + \underset{E}{A}\left\{\tfrac{1}{2}\left[-\tfrac{1}{2}(\boldsymbol{\phi}_{r\bar{E}}\boldsymbol{\eta})\times(\Delta\boldsymbol{\phi}_E\boldsymbol{\eta})\right]^T\right. \\
& \left.\cdot K_E\left[-\tfrac{1}{2}(\boldsymbol{\phi}_{r\bar{E}}\boldsymbol{\eta})\times(\Delta\boldsymbol{\phi}_E\boldsymbol{\eta})\right]\right\} - \tfrac{1}{2}\boldsymbol{u}_2^T K\boldsymbol{u}_2
\end{aligned}
\tag{43}
$$

By the neglecting of the high-frequency corrected modal amplitudes $\boldsymbol{\zeta}'$, the kinematics of the reduced structure model can be expressed as

$$
\boldsymbol{u} = \boldsymbol{\Phi}(\boldsymbol{\theta}' + \boldsymbol{\theta}_2) = \boldsymbol{\Phi}\boldsymbol{\theta}' + \boldsymbol{u}_2 \cong \boldsymbol{\phi}\boldsymbol{\eta}' + \boldsymbol{u}_2 \tag{44}
$$

so that the two quantities that define the elastic behavior of the structure, the elastic energy V [Eq. (43)] and the displacement field $\boldsymbol{u}$ [Eq. (44)], can be expressed as a function of only the low-frequency modes $\boldsymbol{\phi}$ and amplitudes $\boldsymbol{\eta}$, which ensures the numerical efficiency of the proposed method. The three other equations that complete the basic description of the structure are the relationship between $\boldsymbol{u}_2$ and $\boldsymbol{\eta}$ [Eq. (42)], the relationship between $\boldsymbol{\eta}'$, $\boldsymbol{\eta}$, and $\boldsymbol{\eta}_2$ [Eq. (34)], and the relationship between $\boldsymbol{\eta}_2$ and $\boldsymbol{\eta}$, which can be obtained from Eqs. (32) and (42) as

$$
\boldsymbol{\phi}^T K\boldsymbol{\phi}\boldsymbol{\eta}_2 = \boldsymbol{\phi}^T K\boldsymbol{u}_2 \tag{45}
$$

The hypotheses that led to this formulation are summarized as follows.

1) The elastic energy of the structure can be expressed as a quartic function of the configuration variables by means of a second-order corotational formulation or by using the Green–Lagrange tensor (see Sec. III.B).

2) The corotational displacements or the Green–Lagrange strain tensor can be simplified by introducing a generalization of the von Kármán hypothesis: The modal amplitudes corresponding to high-frequency modes are only considered up to first order [see Eq. (25)].

3) The natural frequencies corresponding to nonselected modes are considered to be so high that the effect of the external applied forces projected over the nonselected modes can be considered negligible. Therefore, the high-frequency corrected modal amplitudes $\boldsymbol{\zeta}'$ can be neglected [see Eqs. (41) and (44)]. This is the same hypothesis that allows the variable reduction in the modal analysis.

In the remainder of this section, we will present some ideas and derivations that can help to interpret some aspects of the presented formulation. Because $\boldsymbol{u}_2$ is a quadratic function of $\boldsymbol{\eta}$, it can be interpreted as an extension of the modal expansion up to second-order. The elastic energy can be split into three terms

$$
V = V_l + V_{mh} - V_{mw} \tag{46}
$$

where

$$
\begin{aligned}
V_l &= \tfrac{1}{2}\boldsymbol{\eta}'^T\boldsymbol{\phi}^T K\boldsymbol{\phi}\boldsymbol{\eta}' \\
V_{mh} &= \underset{E}{A}\left\{\tfrac{1}{2}\left[-\tfrac{1}{2}(\boldsymbol{\phi}_{r\bar{E}}\boldsymbol{\eta})\times(\Delta\boldsymbol{\phi}_E\boldsymbol{\eta})\right]^T K_E\left[-\tfrac{1}{2}(\boldsymbol{\phi}_{r\bar{E}}\boldsymbol{\eta})\times(\Delta\boldsymbol{\phi}_E\boldsymbol{\eta})\right]\right\} \\
V_{mw} &= \tfrac{1}{2}\boldsymbol{u}_2^T K\boldsymbol{u}_2
\end{aligned}
\tag{47}
$$

where V_l is a quadratic term, as in the linear case, but now depends on the corrected amplitudes $\boldsymbol{\eta}'$, V_{mh} is a quartic hardening term that for a beam represents the axial extensional elastic energy due to the second-order terms arising from the geometric nonlinearity, and V_{mw} is a quartic weakening term that compensates for the previous one and that for a beam corresponds to the relaxation in the axial extensional energy caused by foreshortening.

The total quartic energy is obtained by subtracting the weakening term from the hardening term

$$
V_m = V_{mh} - V_{mw} \tag{48}
$$

In the case of a plate, the total quartic energy V_m corresponds to the hardening caused by the membrane effect. Therefore, we will sometimes call it generalized membrane energy. It can be demonstrated that V_m is positive semidefinite because it holds that

$$
\begin{aligned}
V_{mh} - V_{mw} = & \underset{E}{A}\left\{\tfrac{1}{2}\left[\boldsymbol{\Phi}_E\boldsymbol{\theta}_2 - \tfrac{1}{2}(\boldsymbol{\phi}_{r\bar{E}}\boldsymbol{\eta})\times(\Delta\boldsymbol{\phi}_E\boldsymbol{\eta})\right]^T\right. \\
& \left.\cdot K_E\left[\boldsymbol{\Phi}_E\boldsymbol{\theta}_2 - \tfrac{1}{2}(\boldsymbol{\phi}_{r\bar{E}}\boldsymbol{\eta})\times(\Delta\boldsymbol{\phi}_E\boldsymbol{\eta})\right]\right\} \geq 0
\end{aligned}
\tag{49}
$$

Another interesting interpretation of the presented theory can be obtained if Eq. (34) is used to define $\boldsymbol{\eta}'$ as a function of $\boldsymbol{\eta}$. Then the

elastic energy consists of a quadratic term V_l plus a hardening term V_w of order higher than four. This suggests that $\boldsymbol{\eta}'$ defines a kinematic description of the structure that maintains a linear behavior of the structure if the quartic hardening term is neglected. The way in which the structure achieves this softened behavior is to curve the linear modes by adding the nonlinear generalized foreshortening $\boldsymbol{u}_2$ to the linear description $\boldsymbol{\phi\eta}'$. This interpretation is closely related to the simplified representation of nonlinear behavior by means of a stress stiffening matrix (Sec. VII.C).

Although in the earlier derivations $\boldsymbol{\zeta}'$ was supposed to be negligible, it can be advantageous to remove this hypothesis in certain cases while maintaning the von Kármán generalized hypothesis. For example, when studying the transversal equilibrium of a rotor blade (Sec. IX.A), it is not necessary to neglect the nonselected modal amplitudes $\boldsymbol{\zeta}'$ corresponding to the axial deformation (in this case the stretch). This is so because the axial equations of equilibrium corresponding to $\boldsymbol{\zeta}'$ are decoupled from the transversal equations corresponding to $\boldsymbol{\eta}$ as far as the elastic energy is concerned [see Eqs. (39) and (40)].

VI. Particularization for a Planar Beam

It will be demonstrated that the earlier defined generalized foreshortening (Sec. IV), which is a general concept valid for structures of any shape, coincides essentially with the traditional concept of foreshortening, which is only applicable to cantilever beams (Sec. II). For this purpose, the same process that led to the attainment of the generalized foreshortening in Sec. IV is particularized in this section for a cantilever beam.

By the use of the same notation as in Sec. II, the elastic energy of the beam can be written as the sum of a term due to the bending V_b plus another term due to the deformation of the neutral fiber V_a:

$$V_b = \frac{1}{2}\int_0^L EI\left(\frac{\partial^2 \boldsymbol{u}_y}{\partial x^2}\right)^2 \mathrm{d}x \tag{50}$$

$$V_a = \frac{1}{2}\int_0^L EA(\varepsilon_{xx0})^2\,\mathrm{d}x$$

$$\varepsilon_{xx0} = \frac{\partial \boldsymbol{u}_x}{\partial x} + \frac{1}{2}\left[\left(\frac{\partial \boldsymbol{u}_x}{\partial x}\right)^2 + \left(\frac{\partial \boldsymbol{u}_y}{\partial x}\right)^2\right] \tag{51}$$

where the Green–Lagrange tensor was used to obtain the axial strain ε_{xx0}.

Because the axial stiffness is usually very high when compared to the bending stiffness, it is assumed that the selected modes of the linear analysis occur in the transverse deflection $\boldsymbol{u}_y$.

If the generalized von Kármán hypothesis defined in Secs. IV and V is applied, the quadratic terms of ε_{xx0} corresponding to the nonselected modes, can be neglected,

$$V_a = \frac{1}{2}\int_0^L EA\left[\frac{\partial \boldsymbol{u}_x}{\partial x} + \frac{1}{2}\left(\frac{\partial \boldsymbol{u}_y}{\partial x}\right)^2\right]^2 \mathrm{d}x \tag{52}$$

The equilibrium equations in the axial direction can be obtained by taking variations with respect to $\boldsymbol{u}_x$ in Eq. (52):

$$EA\frac{\partial}{\partial x}\left[\frac{\partial \boldsymbol{u}_x}{\partial x} + \frac{1}{2}\left(\frac{\partial \boldsymbol{u}_y}{\partial x}\right)^2\right] = f_x, \qquad \boldsymbol{u}_x(0) = 0$$

$$\left[\frac{\partial \boldsymbol{u}_x}{\partial x} + \frac{1}{2}\left(\frac{\partial \boldsymbol{u}_y}{\partial x}\right)^2\right]_{x=L} = 0 \tag{53}$$

where f_x is the applied external force per unit length in the x direction.

Subsequently, the axial displacement $\boldsymbol{u}_x$ is split into the generalized foreshortening $\boldsymbol{u}_{2x}$ (in this case the traditional foreshortening) and the correction displacement $\boldsymbol{u}'_x$ (in this case the stretch):

$$\boldsymbol{u}_x = \boldsymbol{u}'_x + \boldsymbol{u}_{2x} \tag{54}$$

The generalized foreshortening $\boldsymbol{u}_{2x}$ is obtained as the part of $\boldsymbol{u}_x$ arising from the second-order terms in the Green–Lagrange tensor

$$EA\frac{\partial}{\partial x}\left[\frac{\partial \boldsymbol{u}_{2x}}{\partial x} + \frac{1}{2}\left(\frac{\partial \boldsymbol{u}_y}{\partial x}\right)^2\right] = 0, \qquad \boldsymbol{u}_2(0) = 0$$

$$\left[\frac{\partial \boldsymbol{u}_{2x}}{\partial x} + \frac{1}{2}\left(\frac{\partial \boldsymbol{u}_y}{\partial x}\right)^2\right]_{x=L} = 0 \tag{55}$$

and it can be demonstrated by substitution that the solution of Eq. (55) is

$$\boldsymbol{u}_{2x} = -\frac{1}{2}\int_0^L \left(\frac{\partial \boldsymbol{u}_y}{\partial x}\right)^2 \mathrm{d}x \tag{56}$$

which coincides with that of Eq. (3).

VII. Numerical Solution

Some brief guidelines will be given to solve a static analysis problem numerically while following the proposed method. To this end, a set of invariants is calculated at a first preprocessing stage, which are later employed to carry out an iterative analysis of a system of nonlinear equations at a subsequent stage. The underlying formulation of the nonlinear structural analysis to be used is the corotational one already presented (Sec. III) although the results can be easily extended to a Green–Lagrange-tensor-based formulation.

The dynamic algorithm is not included due to space restraints. However, it is easy to derive the expression of the inertia forces from the kinematic description of the structure. In addition, the proposed formulation can be used to generate reduced second-order models of structural components that allow their inclusion in a flexible mechanism. To this end, a floating frame is attached to each structural component, with respect to which the relative displacements are described by the reduced set of modal amplitudes. To reduce the complexity of the formulation, it is advisable to linearize the dependency of the inertia forces on the modal amplitudes whenever it is possible.

A. Equilibrium Equations

The system of nonlinear equilibrium equations can be obtained from the simultaneous effect of the applied forces Q_{ap} and the elastic forces derived from the elastic energy $-\partial V/\partial \boldsymbol{\eta}$:

$$\frac{\partial V}{\partial \boldsymbol{\eta}} = \left(\frac{\partial \boldsymbol{u}}{\partial \boldsymbol{\eta}}\right)^T Q_{\mathrm{ap}} \tag{57}$$

This expression can be expanded using Eqs. (34), (44), and (46–48):

$$\left(I - \frac{\partial \boldsymbol{\eta}_2}{\partial \boldsymbol{\eta}}\right)^T (\boldsymbol{\phi}^T K \boldsymbol{\phi})\boldsymbol{\eta}' + \frac{\partial V_m}{\partial \boldsymbol{\eta}}$$

$$= \left(I - \frac{\partial \boldsymbol{\eta}_2}{\partial \boldsymbol{\eta}}\right)^T \boldsymbol{\phi}^T Q_{\mathrm{ap}} + \left(\frac{\partial \boldsymbol{u}_2}{\partial \boldsymbol{\eta}}\right)^T Q_{\mathrm{ap}} \tag{58}$$

Equation (58) can be further expanded if it is taken into account that both $\boldsymbol{\eta}_2$ and $\boldsymbol{u}_2$ are quadratic functions of $\boldsymbol{\eta}$ [Eqs. (45) and (42)], so that their second derivatives are constant. In addition, V_m is a quartic function of $\boldsymbol{\eta}$, so that its fourth derivatives are constant. By the use of the aforementioned properties and tensorial notation in conjunction with Einstein's notation, Eq. (58) can be rewritten as

$$\left(\delta_{mi} - \frac{\partial^2 \boldsymbol{\eta}_{2m}}{\partial \boldsymbol{\eta}_i \partial \boldsymbol{\eta}_r}\boldsymbol{\eta}_r\right)(K_c)_{mj}\boldsymbol{\eta}'_j + \frac{1}{6}\frac{\partial^4 V_m}{\partial \boldsymbol{\eta}_i \partial \boldsymbol{\eta}_j \partial \boldsymbol{\eta}_k \partial \boldsymbol{\eta}_l}\boldsymbol{\eta}_j \boldsymbol{\eta}_k \boldsymbol{\eta}_l$$

$$= \left(\delta_{mi} - \frac{\partial^2 \boldsymbol{\eta}_{2m}}{\partial \boldsymbol{\eta}_i \partial \boldsymbol{\eta}_r}\boldsymbol{\eta}_r\right)\boldsymbol{\phi}_m^T Q_{\mathrm{ap}} + \left(\frac{\partial^2 \boldsymbol{u}_{2r}}{\partial \boldsymbol{\eta}_i \partial \boldsymbol{\eta}_j}\boldsymbol{\eta}_j\right)^T (Q_{\mathrm{ap}})_r \tag{59}$$

where the condensed stiffness matrix was used,

$$K_c = \boldsymbol{\phi}^T K \boldsymbol{\phi} \tag{60}$$

B. Preprocessing

At this stage the invariants appearing in Eq. (59) can be obtained. The stiffness matrix K and the low-frequency modes ϕ can be calculated by any standard method. The condensed stiffness matrix can also be obtained by applying Eq. (60).

By examination of Eq. (59), it is possible to identify three additional tensors that must be calculated in a preprocessing stage to handle the equilibrium equations effectively. By application of the definitions in Sec. V, they can be obtained as

$$K\left(\frac{1}{2}\frac{\partial^2 \boldsymbol{u}_2}{\partial \boldsymbol{\eta}_i \partial \boldsymbol{\eta}_j}\right) = \mathrm{sym}\left(-\underset{E}{A}\left\{K_E\left(-\frac{1}{2}(\phi_{r\bar{E}})_i \times (\Delta\phi_E)_j\right)\right\}\right) \tag{61}$$

$$\phi^T K \phi\left(\frac{1}{2}\frac{\partial^2 \boldsymbol{\eta}_2}{\partial \boldsymbol{\eta}_i \partial \boldsymbol{\eta}_j}\right) = \phi^T K\left(\frac{1}{2}\frac{\partial^2 \boldsymbol{u}_2}{\partial \boldsymbol{\eta}_i \partial \boldsymbol{\eta}_j}\right) \tag{62}$$

$$\frac{1}{24}\frac{\partial^4 V_m}{\partial \boldsymbol{\eta}_i \partial \boldsymbol{\eta}_j \partial \boldsymbol{\eta}_k \partial \boldsymbol{\eta}_l} = \mathrm{sym}\left(\underset{E}{A}\left\{\frac{1}{2}\left(-\frac{1}{2}(\phi_{r\bar{E}})_i \times (\Delta\phi_E)_j\right)^T \cdot K_E\left(-\frac{1}{2}(\phi_{r\bar{E}})_k \times (\Delta\phi_E)_l\right)\right\}\right) - \left(\frac{1}{2}\frac{\partial^2 \boldsymbol{u}_2}{\partial \boldsymbol{\eta}_i \partial \boldsymbol{\eta}_j}\right)^T K\left(\frac{1}{2}\frac{\partial^2 \boldsymbol{u}_2}{\partial \boldsymbol{\eta}_k \partial \boldsymbol{\eta}_l}\right) \tag{63}$$

where $(\phi_{r\bar{E}})_i$ and $(\Delta\phi_E)_j$ are the columns associated with the modal amplitudes $\boldsymbol{\eta}_i$ and $\boldsymbol{\eta}_j$ in the matrices $\phi_{r\bar{E}}$ and $\Delta\phi_E$. The notation $\mathrm{sym}(x_{ij})$ is used to denote a transformation of the tensor x_{ij} that converts it into a symmetric tensor by averaging terms corresponding to symmetric sets of indexes. The motivation for this transformation is that partial derivatives are symmetric tensors with respects to the indexes of the derivation variables.

C. Stress Stiffening Formulation

In this section a simplified form of the static problem in Sec. VII.A is presented. It corresponds to those approaches that make use of a geometic stiffening matrix. This approach can be considered as being based on the following assumptions.

1) The generalized membrane energy V_m can be neglected,

$$V \cong \tfrac{1}{2}\boldsymbol{\eta}'^T \phi^T K \phi \boldsymbol{\eta}' \tag{64}$$

2) The kinematic field of the structure can be approximated with enough accuracy by a second-order expression in the corrected modal amplitudes $\boldsymbol{\eta}'$. Because the corrected modal amplitudes $\boldsymbol{\eta}'$ and the modal amplitudes $\boldsymbol{\eta}$ are identical up to first-order [see Eqs. (34) and (32)], this is equivalent to replacing in $\boldsymbol{u}$ [Eq. (44)] the dependency of the second-order terms $\boldsymbol{u}_2$ on $\boldsymbol{\eta}$ by a dependency on $\boldsymbol{\eta}'$:

$$\boldsymbol{u} = \phi\boldsymbol{\eta}' + \boldsymbol{u}_2(\boldsymbol{\eta}) \cong \phi\boldsymbol{\eta}' + \boldsymbol{u}_2(\boldsymbol{\eta}') \tag{65}$$

Based on these assumptions, the equilibrium equations [Eq. (59)] can be rewritten as

$$K_c\boldsymbol{\eta}' = \phi^T Q_{\mathrm{ap}} + \left((Q_{\mathrm{ap}})_r \frac{\partial^2 \boldsymbol{u}_{2r}}{\partial \boldsymbol{\eta}^2}\right)\boldsymbol{\eta}'_j \tag{66}$$

where, apart from the linear elastic forces and the projected forces typical of linear formulations, an additional term with a linear dependency on both the applied forces Q_{ap} and the corrected modal amplitudes $\boldsymbol{\eta}'$ appears. This term can be interpreted as the product of the stress stiffness matrix times the corrected modal amplitudes.

This type of formulation is useful when the displacements are small, as in the linear analysis, but the stress stiffening effect cannot be neglected. Clear examples of this are prestressed cables and axially loaded columns. In these cases the stretch or elongation caused by the axial force is negligible. However, the stress stiffening (or weakening) effect produced by the axial force is not negligible. In fact, this effect is either regarded as a design device or as a failure cause. Another case in which this simplified formulation can be applied is the transversal equilibrium of a rotor blade with small deflections (Sec. IX.A).

VIII. Comparison to Other Formulations

Several foreshortening-based formulations in Ref. 9 coincide to a large extent with the one presented here when particularized for the case of a cantilever planar inextensible beam (see Sec. VI). Other derivations in the aforementioned paper do not need the inextensibility assumption and, therefore, give the possibility of calculating the stretch $\psi\boldsymbol{\zeta}'$. In spite of this difference, the results are similar because of the already mentioned decoupling (see Sec. V) between the equations associated with the selected amplitudes $\boldsymbol{\eta}$ and those corresponding to the high-frequency corrected amplitudes $\boldsymbol{\zeta}'$. As a result, if the applied transversal forces do not depend on $\boldsymbol{\zeta}'$ (stretch in beams), the equations for the transverse deflection are the same as in the inextensible case.

The approach by Hanagud and Sarkar[10] can be derived from the presented formulation if the foreshortening projected over the nonselected modes is neglected. For this reason, it requires the selection of a sufficient number of high-frequency modes for the analysis to produce the same compensation of second-order strain that is provided by foreshortening. This causes a growth in the required computational effort not only because of the stiffening of the equations, but also because of the larger number of configuration variables that are required to model the structure. In addition, it is not easy to establish a general criterion that allows one to decide which high-frequency modes need to be included in the analysis for structures other than beams.

The idea of using a geometric stiffness matrix[8,15,16] is roughly equivalent to that of neglecting the quartic energy, and it is very close to the approach presented in Sec. VII.C. However, the approach in Sec. VII.C. is superior in the majority of cases to other approaches to be found in the literature[9] in that they require the external forces to be applied in two stages. First, the external forces (or its most representative term, such as the centrifugal force in the case of a helicopter blade) projected over the high-frequency modes ψ are applied. Afterward, the effect of the forces projected over the low-frequency modes ϕ is calculated introducing the effect of the first-stage forces by means of a stress stiffness matrix. The main disadvantage of these approaches is that they require a judicious selection of the hard modes ψ and representative forces in the first stage, which is not easy to do in cases other than rotating beams.

Similarly, those approaches where the motion is divided into a nominal part and a deviation with respect to it[9] are in essence the same approach as the earlier one, and they also rely heavily on the appropriate definition of the nominal motion.

As for those methods that require the use of modal derivatives,[5,6] their main disadvantage when compared to the proposed approach is that they add the modal derivatives to the base of the configuration space of the structure. For this reason, the number of configuration variables tends to be considerably greater. One way of avoiding this problem would be to use a second-order approximation of the displacements obtained by integrating a second-order approximation of the tangent modes:

$$\boldsymbol{u} \cong \int \phi_t \, \mathrm{d}\boldsymbol{\eta} \cong \int \left(\phi_0 + \left(\frac{\partial \phi_t}{\partial \boldsymbol{\eta}_m}\right)_0 \boldsymbol{\eta}_m\right)\mathrm{d}\boldsymbol{\eta} \tag{67}$$

However, the integral in Eq. (67) is path dependent because the cross-modal derivatives are not equal in general. Therefore, it is not possible to obtain the displacements as a explicit function of $\boldsymbol{\eta}$ and the reduction is less effective.

There is also a connection between the presented formulation and von Kármán's strain-displacement relationships for moderately large-deflection analysis of plates.[13] These relationships can be

obtained by neglecting some terms in the Green–Lagrange strain tensor. The in-plane components of the Green–Lagrange strain tensor on the neutral plane can be expressed as

$$\varepsilon_{xx} = \frac{\partial u}{\partial x} + \frac{1}{2}\left[\left(\frac{\partial u}{\partial x}\right)^2 + \left(\frac{\partial v}{\partial x}\right)^2 + \left(\frac{\partial w}{\partial x}\right)^2\right]$$

$$\varepsilon_{yy} = \frac{\partial v}{\partial y} + \frac{1}{2}\left[\left(\frac{\partial u}{\partial y}\right)^2 + \left(\frac{\partial v}{\partial y}\right)^2 + \left(\frac{\partial w}{\partial y}\right)^2\right]$$

$$\gamma_{xy} = \frac{\partial u}{\partial y} + \frac{\partial v}{\partial x} + \frac{\partial u}{\partial x}\frac{\partial u}{\partial y} + \frac{\partial v}{\partial x}\frac{\partial v}{\partial y} + \frac{\partial w}{\partial x}\frac{\partial w}{\partial y} \tag{68}$$

where the undeformed configuration of the plate occur in the x–y plane and u, v, and w are the displacements in the x, y, and z directions, respectively.

In the linear analysis it is considered that the relevant deformation occurs in the z direction. Consequently, u and v are neglected. On the assumption of small strains, an exact nonlinear formulation can be obtained by employing the Green–Lagrange strain tensor of Eq. (68) at the cost of a considerable complexity in the expression of the strain tensor. However, von Kármán's hypothesis allows us to simplify the analysis by neglecting in Eq. (68) second-order terms in u and v,

$$\varepsilon_{xx} \cong \frac{\partial u}{\partial x} + \frac{1}{2}\left(\frac{\partial w}{\partial x}\right)^2, \qquad \varepsilon_{yy} = \frac{\partial v}{\partial y} + \frac{1}{2}\left(\frac{\partial w}{\partial y}\right)^2$$

$$\gamma_{xy} = \frac{\partial u}{\partial y} + \frac{\partial v}{\partial x} + \frac{\partial w}{\partial x}\frac{\partial w}{\partial y} \tag{69}$$

One way of interpreting von Kármán's-hypothesis is to consider that because the in-plane deformations u and v can be neglected in the linear analysis of plates, in the second-order analysis it is sufficient to include them up to first order as a first approximation of the nonlinear behavior. This hypothesis can then be considered as a particularization of what we called the generalized von Kármán hypothesis in Sec. IV. According to this hypothesis, if either the corotational displacements or the Green–Lagrange tensor are expressed as a function of the modal amplitudes, second-order terms in those modal amplitudes that are neglected in the modal analysis can be considered only up to first order in an approximate nonlinear analysis. Consequently, w can be identified to the selected modal amplitudes and u and v to the nonselected ones.

Simo and Vu-Quoc's formulation of beams and plates[17–20] allows a good representation of geometrically nonlinear behavior by referring the nodal coordinates to an inertial frame. Vu-Quoc and Deng[21] extend these ideas to multilayered beams. If these formulations are compared to the approach proposed in this paper, it can be said that the aforementioned formulations have a wider range of application in terms of the degree of deformation. However, their use is limited to beams and plates, and they are not strictly speaking reduced formulations because the configuration variables are nodal variables. As for the treatment of multilayered beams, the reduced formulation proposed here should be a good approximation for moderate large displacements, even if the corotational approach were used, because a second order approximation of the stretch of the beam caused by bending would be taken into account.

Simo and Vu-Quoc[19] also develop a simplified model of geometrically nonlinear beams and plates (consistent linear equations) by using a zeroth-order approximation of the internal axial force in the case of beams, as explained Sharf.[9] In this sense, this approach can be regarded as an implicit form of the geometric stiffness matrix approach.

IX. Examples

The presented examples are intended to comprise a sufficiently ample number of cases to prove the validity of the formulation. Both static and dynamics problems are studied. To simplify the implementation of the structural formulation, simple four-node elements were used to model the plates in Secs. IX.B and IX.C. As a consequence, the number of finite elements needed to model these structures was sometimes excessive for the capabilities of the hardware available. The precision was, thus, limited by the fineness of the mesh in these examples. For this reason, it is expected that the presented formulation performs even better than the subsequent numerical results show.

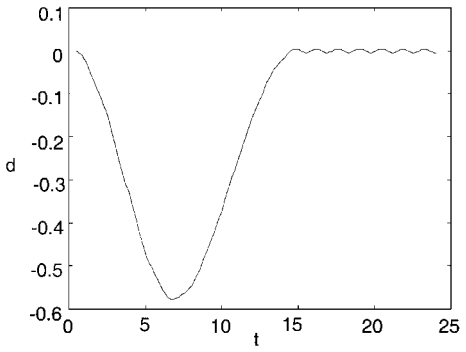

Fig. 4 Tip deflection of the rotating beam.

A. Rotatory Beam

This problem, as mentioned in Sec. II, is the most studied in the literature related to geometric stiffening.[7] For this reason it is appropriate to solve it with the presented method. The mechanical system consists of a cantilever beam, one of whose ends is built into a rotatory axis (see Fig. 1). When an acceleration pulse is applied to this axis, the beam deforms elastically due to the effect of the inertia forces. The angular displacement law[22] is

$$\omega = \omega_s(1/15)[t - (15/2\pi)\sin(2\pi t/15)], \qquad 0 < t < 15$$

$$\omega = \omega_s, \qquad 15 < t < 24 \tag{70}$$

where ω is the angular velocity, t is time, and ω_s is the angular velocity reached in the steady state.

The data of the beam tested by Ider and Amirouche[22] are $E = 7.0e10\ \mathrm{N/m^2}$, $A = 0.0004\ \mathrm{m^2}$, length $= 10$ m, $I = 2.0e{-}7\ \mathrm{m^4}$, $M = 12$ kg, and $\omega_s = 6$ rad/s. To model the beam, the shear energy was neglected, and 10 two-node elements were used. Four modes were selected although good results can be obtained with only one. Figure 4 shows the curve of the transversal tip deformation d vs time t obtained with the proposed formulation, which agrees very well with the results obtained in Refs. 9 and 22.

To obtain the results presented in Fig. 4, the following steps must be followed:

1) The element stiffness matrices K_E, the component stiffness matrix K, the condensed stiffness matrix K_c, and the matrix of selected modes ϕ must be calculated by any standard method.

2) Equation (61) must be used for calculating the constant coefficients of the generalized foreshortening $\partial^2 \boldsymbol{u}_2 / \partial \boldsymbol{\eta}_i \partial \boldsymbol{\eta}_j$.

3) The equations of motion projected over ϕ must be solved for $\boldsymbol{\eta}'$. These equations are the same as in the static case [see Eq. (66)] except that the condensed inertia term $\phi^T M \phi(\mathrm{d}^2\boldsymbol{\eta}'/\mathrm{d}t^2)$ must be included. In addition, the centrifugal inertia force must be included in the generalized forces Q_{ap}. The same equations can be obtained without using inertia forces if a floating frame is used. However, this is not explained in detail for the sake of brevity.

4) The elastic displacement of the tip can be extracted from the elastic displacements $\boldsymbol{u}$ calculated in Eq. (65).

B. Plate with Simply Supported Edges Without In-Plane Slide

This problem is interesting in aeronautics (see Ref. 2), where the hull of an aircraft resists greater stresses than those predicted by the linear theory when the membrane effect comes into play. Figure 5 shows the system studied, which consists of a square plate whose edges have their transverse displacement restricted as well as the in-plane slide perpendicular to themselves. The characteristics of the plate are $E = 7.0e10\ \mathrm{N/m^2}$, h(thickness) $= 0.01$ m, L(side length) $= 10$ m, $\nu = 0.316$, and $\omega_s = 6$ rad/s. The finite element model consists of 10^2 four-node Kirchhoff elements, and the reduced model includes six selected modes.

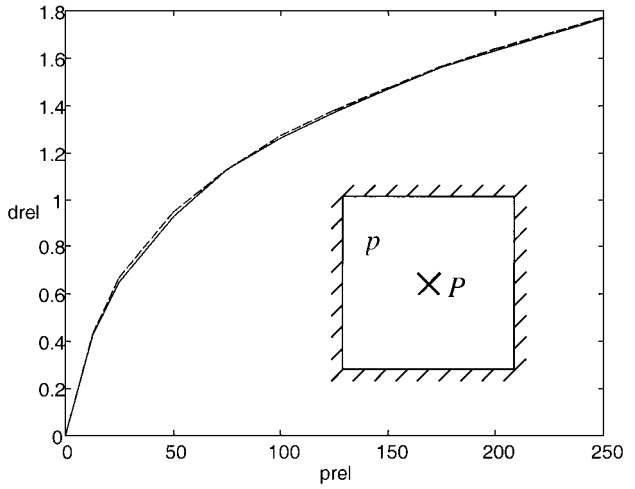

Fig. 5 Center deflection for a plate with simply supported held edges.

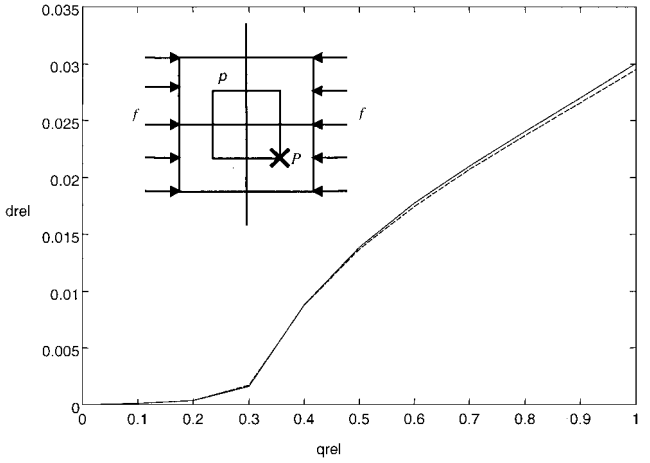

Fig. 6 Inner corner deflection for a plate subjected to in-plane force on opposite edges.

The structure is subjected to uniform pressure p, and as a result, a nonlinear relationship between pressure and deflection is observed. Figure 5 shows the relationship between the relative pressure prel [defined as the quotient $pL^4/(Eh^4)$] and the relative displacement drel (the quotient between the deflection of the plate at the point P in Fig. 5 and the plate thickness h).

The continuous line corresponds to the results provided in Ref. 23, whereas the broken line corresponds to values obtained with the proposed formalism. Both sets of results are in good agreement. However, a finer mesh is expected to improve these results. The shape of these curves suggests that after a short interval of linear behavior the plate becomes more and more stiff as a result of the membrane effect.

To obtain the results presented in Fig. 5, the following steps must be followed.

1) The element stiffness matrices K_E, the component stiffness matrix K, the condensed stiffness matrix K_c, and the matrix of selected modes ϕ must be calculated by any standard method.

2) Equations (61–63) must be used for calculating the constant coefficients of the generalized foreshortening $\partial^2 \boldsymbol{u}_2/\partial\eta_i\partial\eta_j$, the generalized foreshortening projected over the low-frequency modes $\partial^2\eta_2/\partial\eta_i\partial\eta_j$, and the generalized membrane energy $\partial^4 V_m/\partial\eta_i\partial\eta_j\partial\eta_k\partial\eta_l$.

3) The equations of equilibrium [see Eq. (58)] must be solved for $\boldsymbol{\eta}$ [Eq. (34) must be used to express $\boldsymbol{\eta}'$ as a function of $\boldsymbol{\eta}$]. The transverse pressure must be included in the generalized forces Q_{ap}.

4) The transverse elastic displacement of the center of the plate can be extracted from the elastic displacements $\boldsymbol{u}$ calculated in Eq. (44).

C. Buckling of a Plate with a Hole and Simply Supported Edges Subjected to Compressive Forces in Its Plane

In this example the buckling of a square plate with a square hole is studied (see Fig. 6). Apart from the hole, some of the characteristics of the structural system are different from those in Sec.IX.B: $E = 1.0e8$ N/m^2, v $= 0.3$, and L(side length) $= 2$ m. The length of the hole sides is half the length of the plate sides. The plate supports a uniform distribution of compressive force at two opposite sides (see Fig. 6) and no edge can move transversally to the undeformed plane. To avoid the bifurcation uncertainty, a small pressure is applied transversally to the plate.

Figure 6 shows the relationship between the relative force qrel (defined as the quotient between the instantly applied forces and the final maximum ones) vs the relative displacement drel (the quotient between the deflection of the plate at the point P in Fig. 6 and the plate thickness h). The curve shows three different types of behavior: an initial linear interval, a buckling interval where the foreshortening action is noticeable (rapid growth of the deflection), and a final interval where the membrane effect (quartic extensional energy) increases the stiffness of the plate.

The continuous line was obtained with the finite element program ABAQUS,[24] and the broken line represents the results obtained with the proposed formulation. Only a quarter of the plate was modeled for reasons of symmetry. This assumption can be false for buckling, but the example is still valid for testing purposes. The number of finite elements used is $(32^2 - 16^2)$, and the number of selected modes is 8. The ABAQUS model is composed of 12 second-order 9-node square finite elements of type S8R5 with reduced integration, large rotations, and small strains. As for the numeric values of the applied forces, the maximum value of the transverse pressure is 0.2 N/m^2 whereas the maximum value of the compressive force is 2×192 N on each edge.

X. Conclusions

A new formulation is presented that makes it possible to model elastic structures with geometric nonlinearities through the use of a reduced set of variables closely related to the familiar modal amplitudes that are employed in the reduced modal linear structural analysis. The validity of this formulation was tested in a number of examples, which were selected to cover some of the possible fields of application in a simplified way.

The relationships between the proposed formulation and other foreshortening and reduced approaches were also commented on. The proposed formulation proved to offer clear numeric advantages, as well as considerable conceptual value because of the definition and interpretation of concepts such as foreshortening, geometric stiffness, and membrane effect in a common framework, where these concepts were also matched to definite mathematical entities. The formalism explained could also be used to develop new analytical formulas to approximate the behavior of interesting structural members.

Appendix: Least-Squares Calculation of the Element Frame Orientation

If the structure model does not provide orientations, a good substitute $\overline{(\boldsymbol{\Phi}_{rE}\boldsymbol{\theta})}^*$ can be calculated through a least-squares minimization of the following expression for each element E:

$$\min\left(\Delta\boldsymbol{\Phi}_{tE}\boldsymbol{\theta} - \boldsymbol{\theta}^*_{\bar{E}} \times \Delta r_{0E}\right)^T M_E \left(\Delta\boldsymbol{\Phi}_{tE}\boldsymbol{\theta} - \boldsymbol{\theta}^*_{\bar{E}} \times \Delta r_{0E}\right)$$

where $\boldsymbol{\theta}^*_{\bar{E}} = \overline{(\boldsymbol{\Phi}_{rE}\boldsymbol{\theta})}^*$ is the design variable of the minimization process (other symbols are defined in Sec. III). The reason why the least-squares residual is pondered with the mass matrix is to compensate for the approximation being usually finer in those zones where the geometry is more irregular. It must also be taken into account that in finite elements such as those used for modeling thick plates and beams, the rotations provided by the FEM do not represent a mean orientation, but they represent shear deformation, and, hence, a least-square $\boldsymbol{\Phi}_{r\bar{E}}$ must be calculated. For this reason, the most general rule is to calculate a least-squares orientation always.

Acknowledgments

This work was performed under the auspices of the European project Optimal Design and Simulation of Multibody Systems. Support for J. Urruzola was provided by a predoctoral Grant from the Basque government.

References

[1]Vu-Quoc, L., "Dynamics of Flexible Structures Performing Large Overall Motions: A Geometrically-Nonlinear Approach," Ph.D. Dissertation, Univ. of California, Berkeley, CA, May 1986.

[2]Szillard, R., *Theory and Analysis of Plates*, Prentice–Hall, Upper Saddle River, NJ, 1974, pp. 340, 341 and 548, 549.

[3]Timoshenko, S., *Theory of Elastic Stability*, McGraw–Hill, New York, 1936.

[4]Noor, A. K., and Peters, J. M., "Nonlinear Analysis via Global–Local Mixed Finite Element Approach," *International Journal for Numerical Methods in Engineering*, Vol. 15, No. 9, 1980, pp. 1363–1380.

[5]Idelsohn, S. R., and Cardona, A., "A Load-Dependent Basis for Reduced Nonlinear Structural Dynamics," *Computers and Structures*, Vol. 20, Nos. 1–3, 1985, pp. 203–210.

[6]Slaats, P. M. A., De Jongh, J., and Sauren, A. A. H. J., "Model Reduction Tools for Nonlinear Structural Dynamics," *Computers and Structures*, Vol. 54, No. 6, 1995, pp. 1155–1171.

[7]Kane, T. R., Ryan, R. R., and Banerjee, A. K., "Dynamics of a Cantilever Beam Attached to a Moving Base," *Journal of Guidance, Control, and Dynamics*, Vol. 10, No. 2, 1987, pp. 139–151.

[8]Banerjee, A. K., and Lemak, M. E., "Multi-Flexible Body Dynamics Capturing Motion-Induced Stiffness," *Journal of Applied Mechanics*, Vol. 58, Sept. 1991, pp. 766–775.

[9]Sharf, I., "Geometric Stiffening in Multibody Dynamics Formulations," *Journal of Guidance, Control, and Dynamics*, Vol. 18, No. 4, 1995, pp. 882–890.

[10]Hanagud, S., and Sarkar, S., "Problem of the Dynamics of a Cantilever Beam Attached to a Moving Base," *Journal of Guidance, Control, and Dynamics*, Vol. 12, No. 3, 1989, pp. 438–441.

[11]Banerjee, A. K., and Kane, T. R., "Dynamics of a Plate in Large Overall Motion," *Journal of Applied Mechanics*, Vol. 56, Dec. 1989, pp. 887–892.

[12]Cardona, A., and Géradin, M., "Modelling of Superelements in Mechanism Analysis," *International Journal for Numerical Methods in Engineering*, Vol. 32, No. 8, 1991, pp. 1565–1593.

[13]Crisfield, M. A., *Non-Linear Finite Element Analysis of Solids and Structures*, Vols. 1 and 2, Wiley, Sons, New York, 1997, pp. 131–150.

[14]Wu, S. C., and Haugh, E. J., "Geometric Non-Linear Substructuring for Dynamics of Flexible Mechanical Systems," *International Journal for Numerical Methods in Engineering*, Vol. 26, No. 10, 1998, pp. 2211–2226.

[15]Banerjee, A. K., and Dickens, J. M., "Dynamics of an Arbitrary Flexible Body in Large Rotation and Translation," *Journal of Guidance, Control, and Dynamics*, Vol. 13, No. 2, 1990, pp. 221–227.

[16]Wallrapp, O., and Schwertassek, R., "Representation of Geometric Stiffening in Multibody System Simulation," *International Journal for Numerical Methods in Engineering*, Vol. 32, 1991, pp. 1883–1850.

[17]Simo, J. C., and Vu-Quoc, L., "On the Dynamics of Flexible Beams Under Large Overall Motions—The Plane Case: Part I," *Journal of Applied Mechanics*, Vol. 53, No. 4, 1986, pp. 849–854.

[18]Simo, J. C., and Vu-Quoc, L., "On the Dynamics of Flexible Beams Under Large Overall Motions—The Plane Case: Part II," *Journal of Applied Mechanics*, Vol. 53, No. 4, 1986, pp. 855–863.

[19]Simo, J. C., and Vu-Quoc, L., "The Role of Non-Linear Theories in Transient Dynamic Analysis of Flexible Structures," *Journal of Sound and Vibration*, Vol. 119, No. 3, 1987, pp. 487–508.

[20]Simo, J. C., and Vu-Quoc, L., "On the Dynamics in Space of Rods Undergoing Large Motions—A Geometrically-Exact Approach," *Computer Methods in Applied Mechanics and Engineering*, 1988, Vol. 66, No. 2, pp. 125–161.

[21]Vu-Quoc, L., and Deng, H., "Dynamics of Geometrically-Exact Sandwich Beams/1-D Plates: Computational Aspects," *Computer Methods in Applied Mechanics and Engineering*, 1997, Vol. 146, Nos. 1, 2, pp. 135–172.

[22]Ider, S. K., and Amirouche, F. M. L., "Non-Linear Modelling of Flexible Multibody Systems Dynamics Subjected to Variable Constraints," *Journal of Applied Mechanics*, Vol. 56, No. 2, 1989, pp. 444–450.

[23]Young, W. C., *Roark's Formulas for Stress and Strain*, McGraw–Hill, New York, 1989, p. 480.

[24]"ABAQUS/Standard User's Manual," Hibbit, Karlsson, and Sorensen, Hibbit, Karlsson, and Sorensen, Inc., Pawtucket, RI, 1994.